Supporting Information

Gregorian et al. 10.1073/pnas.0910398106

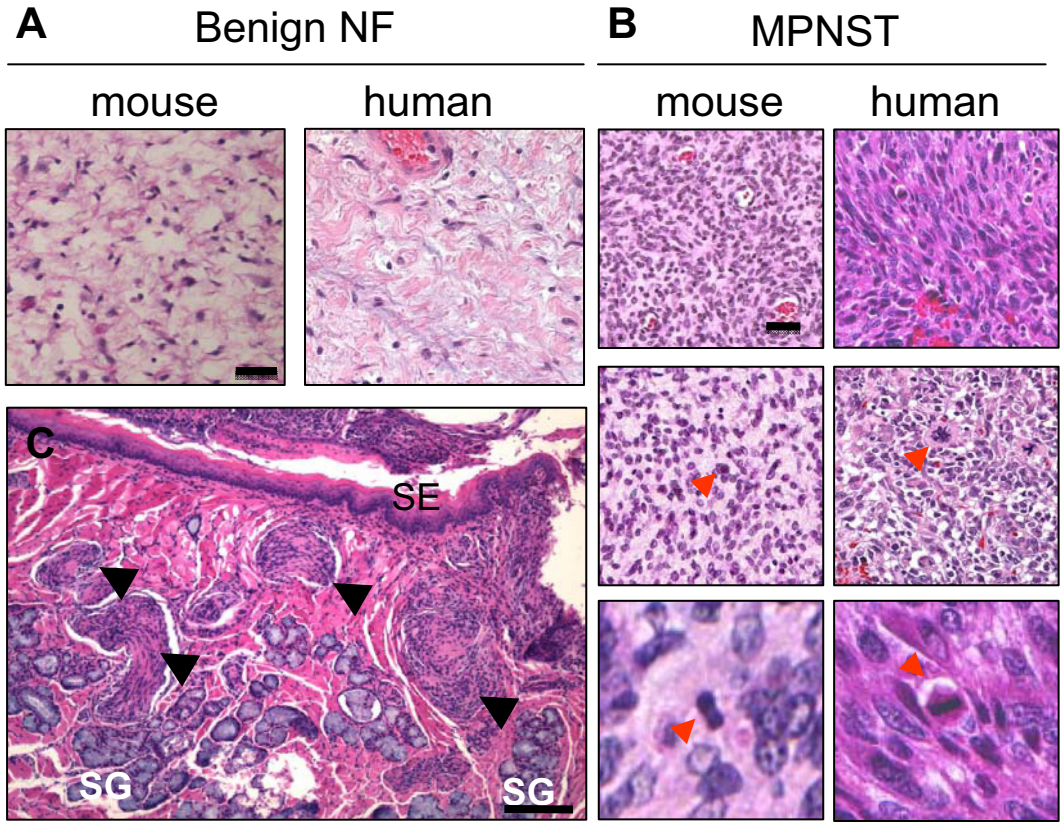

Fig. S1. Histopathological comparison of human NF1 and NF1-associated MPNST lesion with that *mGFAP-Cre*$^{+}$;*Pten*$^{loxp/+}$;*LSL-K-ras*$^{G12D/+}$ model. Representative tumors were subjected to histopathological analysis, which reveals the presence of (*A*) benign NF (scale bar, 25 mm) and (*B*) MPNSTs. MPNST tumors have increased cellularity (*B*, top), cellular anaplasia (middle, nuclear pleomorphism; arrowheads with an adjacent atypical mitosis; (scale bar, 25 mm), and obvious mitoses (bottom, arrowheads). (*C*) H&E stain of *mGFAP-Cre*$^{+}$;*Pten*$^{loxp/+}$;*LSL-K-ras*$^{G12D/+}$ mouse tumor revealed multiple microscopic tumor nodules (arrows), which resemble clinical classification as plexiform NFs. (Scale bar, 155 mm.) SE, squamous epithelium; SG, salivary glands.

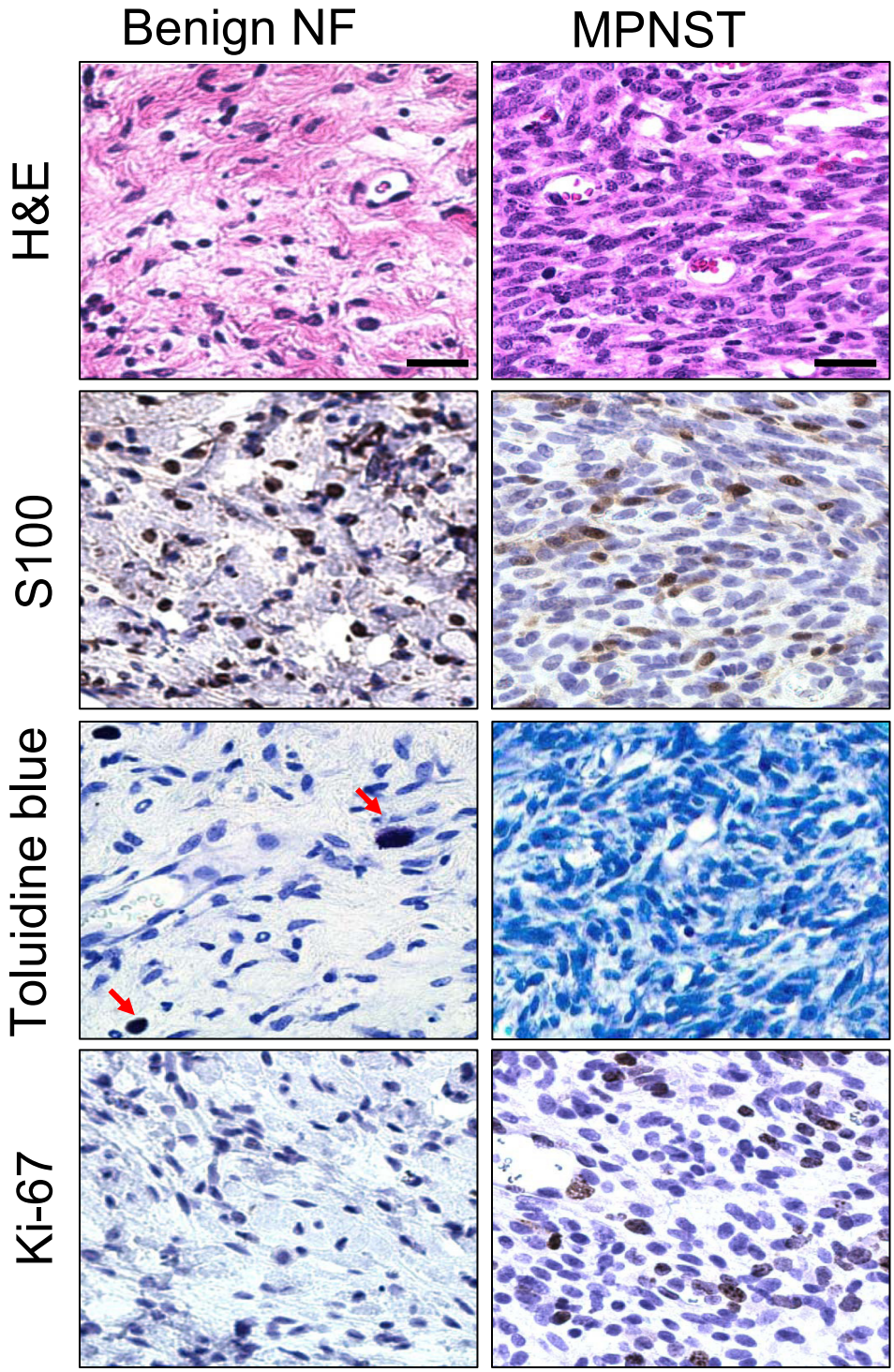

Fig. S2. Characterization of NF (benign NF) and MPNST lesions (top panels) of *mGFAP-Cre*$^{+}$;*Pten*$^{loxp/+}$;*LSL-K-ras*$^{G12D/+}$ mutant mice revealed S100 staining of Schwann cells (second panels), toluidine stained mast cells (third panels), and staining for proliferation marker Ki-67 (lower panels). (Scale bars, 20 mm.) NFs show more diffuse S100 staining, increased numbers of mast cells, and a reduced Ki-67 rate compared to MPNSTs.

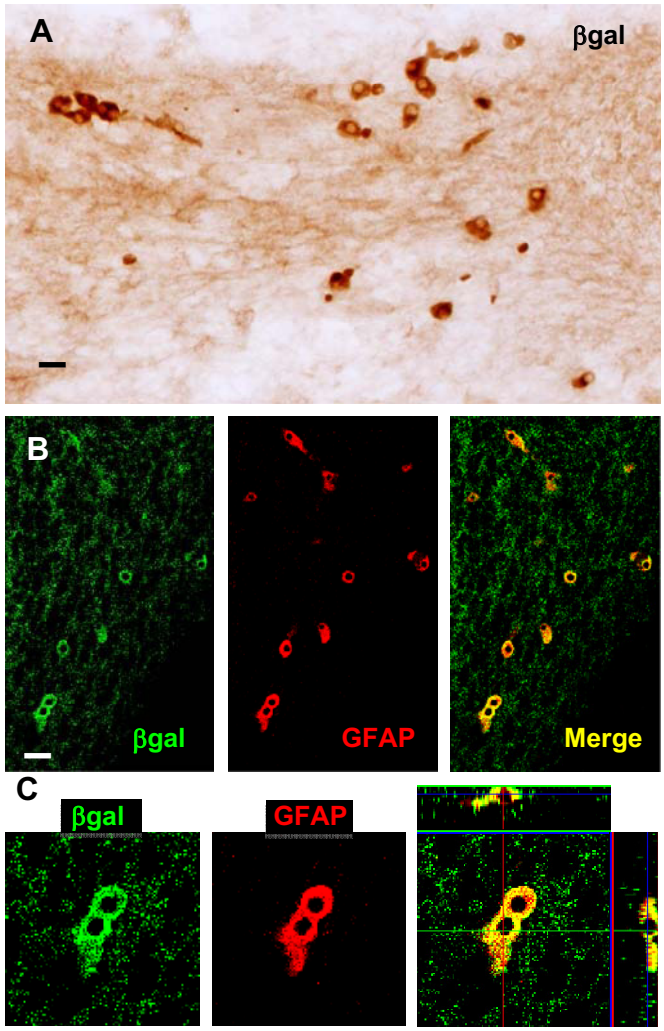

Fig. S3. mGFAP-Cre expression completely overlaps with the endogenous GFAP expression pattern. (*A*) Anti-β-gal IHC-stained sections were examined and photographed using bright field microscopy; (*B*) a consecutive section was co-stained with anti-β-gal and anti-GFAP antibodies and photographed using fluorescence microscopy (Zeiss) and scanning confocal laser microscopy (Leica) to show complete overlapping expressions of both markers. (*C*) High power images of panel *B*.

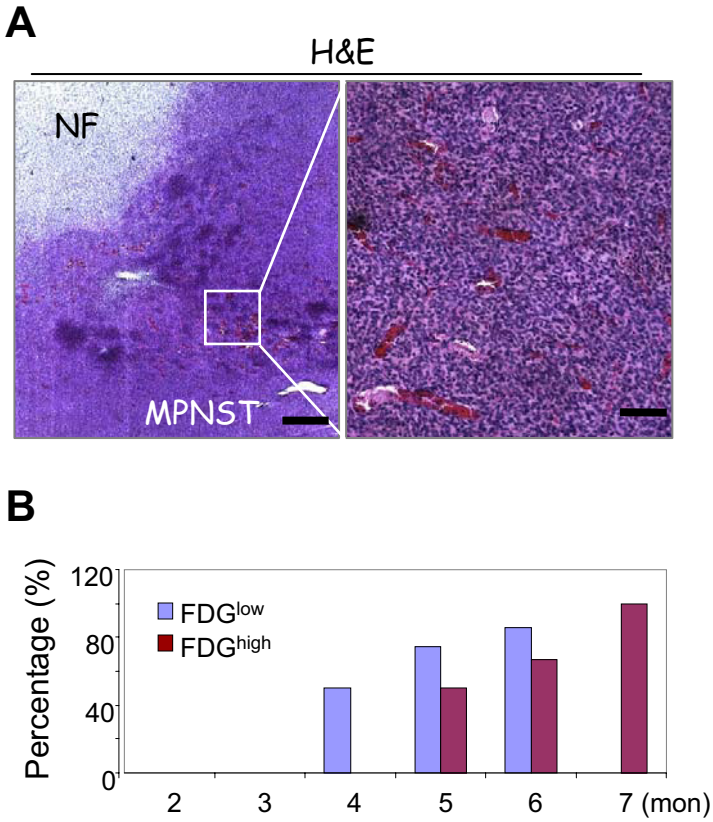

Fig. S4. (*A*) H&E stained section shows increased angiogenesis in MPNST lesions. (*B*) Percentages of animals with detectable FDG^{low} and FDG^{high} lesions.